Short-term salt stress reduces photosynthetic oscillations under triose phosphate utilization limitation in tomato

Zhang, Yuqi; Kaiser, Elias; Dutta, Satadal; Sharkey, Thomas D.; Marcelis, Leo F.M.; Li, Tao

DOI
10.1093/jxb/erae089

Publication date
2024

Document Version
Final published version

Published in
Journal of Experimental Botany

Journal of Experimental Botany, Vol. 75, No. 10 pp. 2994–3008, 2024
https://doi.org/10.1093/jxb/erae089 Advance Access Publication 4 March 2024

RESEARCH PAPER

Short-term salt stress reduces photosynthetic oscillations under triose phosphate utilization limitation in tomato

Yuqi Zhang[1], Elias Kaiser[2], Satadal Dutta[3], Thomas D. Sharkey[4,5,6], Leo F. M. Marcelis[2], and Tao Li[1,*]

[1] Institute of Environment and Sustainable Development in Agriculture, Chinese Academy of Agricultural Sciences, Beijing, China
[2] Horticulture and Product Physiology, Department of Plant Sciences, Wageningen University, Wageningen, the Netherlands
[3] Department of Precision and Microsystems Engineering, Faculty of 3ME, TU Delft, Delft, the Netherlands
[4] MSU-DOE Plant Research Laboratory, East Lansing, MI 48824, USA
[5] Department of Biochemistry and Molecular Biology, Michigan State University, East Lansing, MI 48824, USA
[6] Plant Resilience Institute, Michigan State University, East Lansing, MI 48824, USA

* Correspondence: litao06@caas.cn

Received 29 November 2023; Editorial decision 28 February 2024; Accepted 2 March 2024

Editor: Ian Dodd, Lancaster University, UK

Abstract

Triose phosphate utilization (TPU) limitation is one of the three biochemical limitations of photosynthetic CO_2 assimilation rate in C_3 plants. Under TPU limitation, abrupt and large transitions in light intensity cause damped oscillations in photosynthesis. When plants are salt-stressed, photosynthesis is often down-regulated particularly under dynamic light intensity, but how salt stress affects TPU-related dynamic photosynthesis is still unknown. To elucidate this, tomato (*Solanum lycopersicum*) was grown with and without sodium chloride (NaCl, 100 mM) stress for 13 d. Under high CO_2 partial pressure, rapid increases in light intensity caused profound photosynthetic oscillations. Salt stress reduced photosynthetic oscillations in leaves initially under both low- and high-light conditions and reduced the duration of oscillations by about 2 min. Besides, salt stress increased the threshold for CO_2 partial pressure at which oscillations occurred. Salt stress increased TPU capacity without affecting Rubisco carboxylation and electron transport capacity, indicating the up-regulation of end-product synthesis capacity in photosynthesis. Thus salt stress may reduce photosynthetic oscillations by decreasing leaf internal CO_2 partial pressure and/or increasing TPU capacity. Our results provide new insights into how salt stress modulates dynamic photosynthesis as controlled by CO_2 availability and end-product synthesis.

Keywords: Dynamic light, gas exchange, salt stress, tomato, TPU limitation, triose phosphate utilization.

Introduction

Triose phosphate utilization (TPU) limitation is one of the three biochemical limitations of steady-state photosynthetic carbon assimilation rate (A) in C_3 plants, along with ribulose 1,5-bisphosphate carboxylase/oxygenase (Rubisco) limitation and ribulose-bisphosphate (RuBP) regeneration limitation (Sharkey *et al.*, 2007). During photosynthesis, plants fix CO_2 from

the atmosphere onto RuBP, producing 3-phosphoglycerate, which is reduced to triose phosphates (TPs) (Szecowka *et al.*, 2013). TPs are dephosphorylated during RuBP regeneration and end-product synthesis (mainly for starch and sucrose), and inorganic phosphates (P_i) are released (Sharkey *et al.*, 1986). P_i is required by ATP synthase to produce ATP to sustain the Calvin–Benson–Bassham (CBB) cycle. When increased light intensity and CO_2 partial pressure ($[CO_2]$) increase A to high rates, end-product synthesis from TPs can become slower than TP production in the CBB cycle, transiently decreasing available P_i, and limiting A to the rate of TPU. In other words, how fast TPs are converted to end products limits maximum steady-state photosynthetic capacity. TPU capacity is flexible and can acclimate to environmental conditions (McClain and Sharkey, 2019), such as $[CO_2]$, light intensity, temperature, and abiotic stresses (Yang *et al.*, 2016; McClain and Sharkey, 2019; Rogers *et al.*, 2021).

When A is TPU limited or close to TPU limitation, any larger perturbation could cause damped oscillations in A that last several minutes until reaching a new steady state (Fig. 1). Step increases in light intensity or $[CO_2]$, as well as reductions in O_2 partial pressure ($[O_2]$) (McVetty and Canvin, 1981; Ogawa, 1982; Walker *et al.*, 1983; Sharkey *et al.*, 1986), cause this phenomenon. Such oscillations in A have been observed for over 80 years, and were accompanied by oscillations in chlorophyll fluorescence (Walker *et al.*, 1983; Stirbet *et al.*, 2014), photosystem I oxidation state (McClain and Sharkey, 2023), light scattering (Sivak *et al.*, 1985), pool sizes of photosynthetic intermediates (Sage *et al.*, 1988), pH in the chloroplast stroma (Fridlyand, 1998), ATP/ADP and NADPH/NADP ratios (Walker, 1992), and isoprene emissions (Rasulov *et al.*, 2016). Many researchers proposed that understanding these oscillations equates to understanding the regulation of photosynthesis, as this oscillatory behavior provides a way to analyse feedbacks among electron transport, photophosphorylation, CBB cycle, and end-product synthesis (Laisk *et al.*, 1991; Walker, 1992; Dietz and Hell, 2015). Several mechanisms could explain oscillations in photosynthesis: (i) an imbalance in the supply of ATP and NADPH to the CBB cycle (Ogawa, 1982; Laisk *et al.*, 1991); (ii) a delay originating from sucrose phosphate synthase (SPS) and cytosolic fructose-2,6-bisphosphate, controlling the rate of sucrose synthesis (Stitt *et al.*, 1984; Laisk and Walker, 1986; Laisk and Eichelmann, 1989; Laisk *et al.*, 1989) (iii) slow sugar transport between mesophyll cells (Siebke and Weis, 1995); (iv) independent changes in stromal ATP/ADP and in proton gradient of the thylakoid membrane (ΔpH) (Fridlyand, 1998); and (v) slow kinetics of adenylate turnover in the CBB cycle (Giersch, 1986). Several hypotheses were tested using mathematical models (Giersch, 1986; Laisk and Walker, 1986; Laisk *et al.*, 1991), in which photosynthesis oscillations were caused through arbitrary delays somewhere in the CBB cycle, sucrose synthesis, or electron and proton transport, with steady-state A overshooting before inhibition was achieved. Regardless of these different hypotheses, there is general consensus that A does not start oscillating unless it suddenly enters TPU limitation as it needs a high $[CO_2]$, and that a lack of ATP causes troughs in the oscillation (Laisk *et al.*, 1991; Rasulov *et al.*, 2016; McClain and Sharkey, 2023).

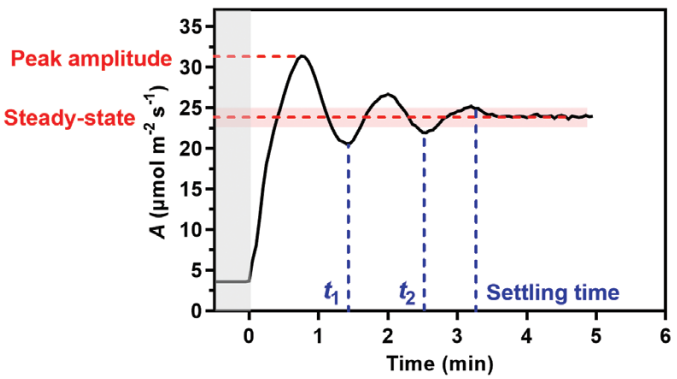

Fig. 1. Example of damped photosynthetic oscillation in a tomato leaf after an increase from a low light intensity (50 μmol m^{-2} s^{-1}; shaded area) to a high light intensity (1000 μmol m^{-2} s^{-1}; at time=0) under saturating CO_2 concentration. Key oscillatory parameters derived from the curve are shown, including peak amplitude, steady-state value, and settling time. Settling time is reached when photosynthetic rate (A) has fallen to within ±5% (indicated as the light red bars) of the final steady-state value. t_1 and t_2 are the time of first and second trough.

In nature, leaves often experience highly dynamic light intensities, as solar angle, cloud movement, wind-induced leaf fluttering, and shading from overlapping leaves and neighboring plants vary (Schurr *et al.*, 2006; Kaiser *et al.*, 2018). Suddenly exposing a shaded leaf to a high light intensity requires a few seconds to tens of minutes to reach steady-state A (Van der Veen, 1949; Kaiser *et al.*, 2017a). This process is called photosynthetic induction, and is transiently limited by (changes in) CBB cycle intermediate pool sizes, Rubisco activation state, stomatal and mesophyll conductance, and (in rare cases) the rate of end-product synthesis (Furbank and Walker, 1985; Kaiser *et al.*, 2015; Liu *et al.*, 2022). After a long period of darkness or shade at intermediately high $[CO_2]$ (>800 μbar), measuring photosynthetic induction demonstrated an overshoot of A, followed by a single reduction before reaching a steady state, in a diverse range of species (e.g. chrysanthemum, lettuce, tomato, and wheat) (Kaiser *et al.*, 2017b; Salter *et al.*, 2019; N. Zhang *et al.*, 2022). The transient decrease in A is reported to be mainly due to low activity in sucrose synthesis (Stitt and Grosse, 1988). After a long period of darkness or shade, SPS activity could be low in the above species. When light intensity suddenly increases, the transient overshoot of CO_2 carboxylation drains the inorganic P_i pool quickly, with delayed activation of SPS causing the CBB cycle to be transiently P_i-limited (Stitt and Grosse, 1988).

Salt stress, induced by soil salinity, is a major abiotic stress in crop production, and strongly decreases A (Chaves *et al.*, 2011). By decreasing stomatal conductance (g_s), salt stress impairs the diffusion of CO_2 towards Rubisco. Salt stress can also impair

electron transport, ATP synthesis, CO_2 carboxylation, and RuBP regeneration (Wungrampha *et al.*, 2018; Zorb *et al.*, 2019). In nature, plants often experience salt stress concomitant with highly dynamic light intensities. We previously demonstrated that photosynthetic induction under dynamic light was strongly inhibited in salt-stressed tomato leaves, when photosynthetic capacity had not yet been down-regulated (Zhang *et al.*, 2018; Y. Zhang *et al.*, 2022). However, we still lack knowledge on how dynamic photosynthesis in salt stressed leaves is regulated when g_s does not limit A, particularly under high [CO_2]. A short-term (7 d) salt stress treatment increased TPU capacity in tomato leaves, without affecting maximum CO_2 carboxylation and electron transport rates (Y. Zhang *et al.*, 2022). An increase in end-product synthesis capacity (e.g. sucrose and/or starch synthesis) relative to CO_2 carboxylation or electron transport might increase TPU capacity (Yang *et al.*, 2016; McClain and Sharkey, 2019). Investigating photosynthetic oscillations under high [CO_2] could help in understanding how salt stress regulates TPU under dynamic light. Also, a diverse range of oscillation data could provide novel insights on the mechanisms behind A oscillations.

This study aimed to investigate whether and how salt stress affects photosynthetic oscillations under TPU limitation. This knowledge may help further understand how salt stress regulates photosynthesis. Tomato (*Solanum lycopersicum*) was used, as it is a C_3 model species, an important crop, and a major fruit vegetable globally. To address the above question, tomato plants were treated with or without salt stress. Leaf acclimation traits to short-term salt stress, and steady-state and dynamic photosynthesis under ambient and high [CO_2] were investigated.

Materials and methods

Plant material and growth conditions

Tomato (*Solanum lycopersicum* cv. Moneymaker) seeds were germinated in stonewool plugs (Grodan, Roermond, the Netherlands), and transferred to stonewool cubes (10 cm×10 cm×7 cm; Grodan) upon unfolding of the second true leaf. Plants were grown in a growth chamber with a photoperiod (day/night) of 16/8 h and ambient CO_2 partial pressure. Day/night temperature was 23/20 °C, and average relative humidity was 75%. Plants were subjected to 200 μmol m^{-2} s^{-1} photosynthetic photon flux density (PPFD) measured at the top of the canopy. PPFD was provided by fluorescent tube lights (Philips, China).

After 6 d of transplanting to stonewool cubes, plants were divided into two groups, which were allocated to two treatments: 0 and 100 mM NaCl treatments were applied for 13 d. Plants in non-stress treatments (0 mM NaCl) were irrigated with nutrient solution for tomato (electrical conductivity (EC)≈2.1 dS m^{-1}, pH≈5.5; Kaiser *et al.*, 2017a). For salt-stress treatments, 100 mM of NaCl was added to the nutrient solution (EC≈12 dS m^{-1}, pH≈5.5). Plants were irrigated every 2–3 d, allowing abundant leaching of excess nutrient solution to maintain a stable salt content in the root zone. To avoid position effects on plant growth, plants were rotated randomly daily. During the 10th–13th day after the start of the salt stress treatment, the third true leaves, counting from the bottom of the plant (the youngest fully expanded leaves), were used for measurements. The experiment was repeated six times in succession, with six to eight plants per treatment and experiment. Except for protein phosphorylation analysis (which was conducted in one experiment only), the following measurements were repeated in two independent experiments (i.e. two blocks), though not all measurements were done in each experiment. The number of replicates of each measurement is specified in the figure captions.

Gas exchange and chlorophyll fluorescence

Photosynthetic gas exchange and chlorophyll fluorescence measurements were performed using the LI-6800 photosynthesis system (LI-COR Biosciences, Lincoln, NE, USA), equipped with a leaf chamber fluorometer (LI-COR, 6800-01A, enclosed leaf area: 2 cm^2). All measurements were performed at a leaf temperature of approximately 23 °C, leaf-to-air vapor pressure deficit of 0.7–1.0 kPa (except during a sudden increase in light intensity), and flow rate of air through the chamber of 500 μmol s^{-1}. Irradiance was provided by a mixture of red (90%) and blue (10%) LEDs in the fluorometer. Peak intensities of red and blue LEDs were at wavelengths of 625 and 475 nm, respectively.

Light and CO_2 response curves of leaf photosynthesis

Leaves were dark-adapted for approximately 30 min, and gas exchange parameters together with minimal (F_o) and maximal (F_m) chlorophyll fluorescence were recorded to determine the maximum quantum efficiency of photosystem II photochemistry (F_v/F_m). PPFD was then increased in steps of 50, 100, 150, 250, 400, 600, 800, 1000, and 1200 μmol m^{-2} s^{-1}. Upon reaching steady-state conditions at each PPFD (10–15 min), gas exchange and chlorophyll fluorescence parameters were logged. Fluorescence yields under actinic light (F_s) and maximum (F_m') fluorescence were recorded with a multiphase flash (MPF) chlorophyll fluorescence routine (for detailed information on this technique, refer to Loriaux *et al.* 2013). Settings of the MPF for tomato leaves were determined in a preliminary experiment: the measuring beam intensity was 1 μmol m^{-2} s^{-1}, maximum flash intensity was 7000 μmol m^{-2} s^{-1}, flash intensity decreased by 60% during the second phase of the MPF, and the durations of the three flash phases were 300, 650, and 400 ms. The quantum efficiency of photosystem II photochemistry (Φ_{PSII}) and non-photochemical quenching (NPQ) were calculated accordingly.

Leaves were adapted in the LI-6800 leaf chamber to 1000 μmol m^{-2} s^{-1} PPFD and 400 μbar CO_2, until A was stable. Leaves were then exposed to a range of CO_2 partial pressures (400, 300, 200, 150, 100, 70, 50, 30, 400, 600, 800, 1000, 1200, 1500 μbar). Upon reaching steady-state conditions at each CO_2 partial pressure (duration was 3–5 min per step, except the step from 50 to 400, which took ~15 min), gas exchange along with chlorophyll *a* fluorescence was logged.

A non-rectangular hyperbolic function (Cannell and Thornley, 1998) was fitted to the light response curve, and parameters were derived, including maximum net photosynthetic rate (A_{max}), dark respiration rate (R_{dark}), and apparent quantum yield (α). Day respiration rate (R_d) was estimated to be 50% of R_{dark} (Sharkey, 2016). Mesophyll conductance (g_m) at 400 μbar CO_2 and 1000 μmol m^{-2} s^{-1} PPFD was calculated using the variable J method (Harley *et al.*, 1992). Using measured A–C_i curve values and fixed R_d and g_m values, maximum carboxylation rate (V_{cmax}), electron transport rate at 1000 μmol m^{-2} s^{-1} PPFD (J_{1000}), and TPU were derived, using the Microsoft Excel solver provided by Sharkey (2016).

Dynamic photosynthetic responses to step changes in irradiance

Four distinct protocols were used to probe dynamic photosynthesis responses to step changes in light intensity. Measurements were conducted in fully shade-adapted leaves in protocols 1 and 2, and in fully high light-adapted leaves in protocols 3 and 4. In protocols 3 and 4, we also intended to study how shadefleck duration and [CO_2] affected dynamic

photosynthesis in both salt-stressed and non-stressed plants. During all measurements, gas exchange was logged every 3 s.

Protocol 1

Plants were adapted in a dark room for ~30 min. Selected leaflets were placed in the LI-6800 cuvette, and F_o and F_m were recorded. Thereafter, light in the room was switched on, PPFD in the cuvette was then increased to 50 μmol m^{-2} s^{-1}, and leaves were adapted at this PPFD until A and g_s were at a steady-state (approx. 30 min). After that, PPFD was increased in a single-step change to 1000 μmol m^{-2} s^{-1} for 20 min. To analyse chlorophyll fluorescence parameters, another set of induction time courses was measured on different leaves, with the same environmental conditions as described above. F_s and F_m' were logged every minute. All measurements were performed at two different [CO_2], namely 400 and 1500 μbar.

Protocol 2

Plants were adapted in a dark room for ~30 min. Selected leaflets were placed in the LI-6800 cuvette, and F_o and F_m were recorded. Thereafter, light in the room was switched on, PPFD in the cuvette was then increased in a single-step to 50 μmol m^{-2} s^{-1} for 9 min. Then, leaves were subjected to five cycles of 3 min of high (1000 μmol m^{-2} s^{-1}) followed by 3 min of low (50 μmol m^{-2} s^{-1}) PPFD. Chlorophyll fluorescence measurements were performed on different leaves, with the same environmental conditions as described above. F_s and F_m' were logged every minute. All measurements were performed at two different [CO_2], namely 400 and 1500 μbar.

Protocol 3

Leaves were exposed to PPFD of 1000 μmol m^{-2} s^{-1} and [CO_2] of 1500 μbar, until A was stable. After that, PPFD was decreased to 50 μmol m^{-2} s^{-1} for shadeflecks of 1, 3, 5, or 10 min duration. Then, PPFD was returned to 1000 μmol m^{-2} s^{-1}, until A was stable.

Protocol 4

Leaves were exposed to PPFD of 1000 μmol m^{-2} s^{-1} and [CO_2] of 400, 600, 800, 1000, 1200, or 1500 μbar, until A was stable. After that, PPFD was decreased to 50 μmol m^{-2} s^{-1} for shadeflecks of 1 min duration. Then, PPFD was returned to 1000 μmol m^{-2} s^{-1}, until A was stable.

Parameter estimation

From transient A, we extracted the following parameters (Fig. 1): (i) peak amplitude in A: amplitude of the first maximum value of A (overshoot), during photosynthetic oscillation; (ii) steady-state A: steady-state A at PPFD of 1000 μmol m^{-2} s^{-1}, calculated as mean value over 60 s after the last oscillation had ended; (iii) settling time: the time when A fell to within ±5% of the final steady-state value; and (iv) oscillation frequency: calculated as $1/(t_2-t_1)$, where t_1 and t_2 were the time of the first and second trough, respectively.

Specific leaf area

After 13 d of salt stress treatment, fresh weight and leaf area of the third true leaves were determined. After leaves were dried at 80 °C for 3 d, their dry weights were measured. Specific leaf area (SLA) on a dry weight basis was calculated.

Soluble sugar and starch contents

On day 13 at noon after the salt stress treatment, the third true leaves were collected, immediately plunged into liquid nitrogen, and stored at −80 °C.

Frozen samples (0.3 g) were extracted with 80% ethanol in a water bath (80 °C for 30 min). The supernatants were dried with a sample concentrator (DC150-1A; Yooning Instrument Co., Hangzhou, China), and dissolved with 50% acetonitrile solution. Sucrose, glucose, and fructose concentrations in the solution were analysed with ultra-performance liquid chromatography (Acquity H-Class; Waters, Milford, MA, USA) using a refractive index detector as described by Dartora *et al.* (2011). The sediments remaining after ethanolic extraction were added with ultra-pure water and gelatinized in a water bath (100 °C for 15 min). Afterwards, starch was enzymatically converted to glucose by thermostable α-amylase at 55 °C and by amyloglucosidase at 60 °C, and measured as soluble sugars, as described above.

Sucrose-phosphate synthase content

Frozen samples (~0.1 g) were used to determine SPS content. SPS content was assayed using an ELISA kit (Beijing Welab Biotechnology Co., Ltd, Beijing, China) following the manufacturer's instructions. Total protein content was measured using the commercial bicinchoninic acid kit (Beijing Welab Biotechnology Co., Ltd) following the manufacturer's instructions. SPS content was calculated on both leaf area basis and total protein basis.

Protein phosphorylation analysis

Proteins were extracted using the phenol extraction method (Yue *et al.*, 2020). The concentrations of the protein extracts were determined with the bicinchoninic acid method (BCA Protein Assay kit; Thermo Fisher Scientific, Waltham, MA, USA). Approximately 10 μg total protein was separated using 12% SDS-PAGE, and the gel was visualized by Coomassie brilliant blue stain. According to the measured protein concentration, the same quantity of protein was taken from each sample and was diluted to the same concentration and volume. For digestion, proteins were reduced with dithiothreitol modified with iodoacetamide, and digested with trypsin (Hua Lishi Scientific, Beijing, China) in 50 mM ammonium bicarbonate for 14 h at 37 °C. Peptides were labeled with TMT 6 reagent (cat. no. 90066, Thermo Fisher Scientific). The peptide mixture was purified and desalted on C18 SEP-Pak columns (Waters). Phosphopeptides were enriched using the IMAC Phosphopepetide enrichment kit (cat. no. A32992, Thermo Fisher Scientific). The enriched peptides were used for a LC-MS/MS scan on a Q Exactive HF mass spectrometer (Thermo Fisher Scientific) and EASY-nLCTM 1200 system (Thermo Fisher Scientific). LC-MS/MS raw data were imported into MaxQuant (version 1.6.17.0) for analysis. The log2-transformed intensity of five SPS phosphopeptides (SPS S150, SPS S700, SPSB S147, SPSB S157, and SPSB S715) was extracted, and Student's t-test with a P-value cutoff of <0.05 was carried out to test for differences between the treatments.

Statistical analysis

One-way ANOVA in randomized blocks (experiments as blocks) was performed to test the differences between treatments. All analyses were performed using Genstat 20th edition (VSN International, Hemel Hempstead, UK).

Results

Dynamic responses of leaf photosynthesis to changes in irradiance under ambient and high CO_2 partial pressures

Under [CO_2] of 400 μbar, salt stress reduced the rate of photosynthetic induction in shade-adapted leaves, though final

A was similar between treatments (Fig. 2A). Salt stress significantly decreased initial g_s compared with control leaves, but after 20 min of high light exposure, the initial difference between treatments was reduced (Fig. 2B). Leaf internal CO_2 partial pressure (C_i) in both treatments showed an initial drop, with a larger amplitude in salt-stressed leaves (Fig. 2C). Thereafter, C_i gradually increased and remained constant, with similar levels in both treatments (Fig. 2C). Φ_{PSII} and NPQ showed similar values between treatments during induction at 400 μbar (Fig. 2D, E).

Under [CO_2] of 1500 μbar, A in both treatments showed large oscillations during the first 10 min of induction, but these stopped earlier in salt-stressed leaves (Fig. 2F). No oscillations were observed in g_s, but they were visible in C_i, Φ_{PSII}, and NPQ (Fig. 2G–J). Salt stress decreased g_s and C_i constantly (Fig. 2G, H). Also, salt stress reduced g_s upon high [CO_2] more strongly compared with control leaves (Fig. 2B, G). Salt-stress increased Φ_{PSII} transiently compared with control leaves, and decreased NPQ compared with control (Fig. 2I, J).

Under a series of light- and shadeflecks, salt stress strongly affected leaf gas exchange and chlorophyll fluorescence (Fig. 3). Under [CO_2] of 400 μbar, salt stress dramatically reduced photosynthetic induction, especially during the first and second lightflecks (Fig. 3A). g_s and C_i showed similar patterns during lightflecks as during photosynthetic induction (Fig. 3B, C). Contrastingly, under [CO_2] of 1500 μbar, during each lightfleck, A showed oscillations with two peaks and one trough between peaks (Fig. 3F). Interestingly, salt stress largely increased the height of the trough during each lightfleck, meaning that oscillations in salt-stressed leaves were more strongly dampened compared with control leaves (Fig. 3F). g_s and C_i showed similar patterns during lightflecks as during photosynthetic induction (Fig. 3G, H). Φ_{PSII} and NPQ also showed oscillations under lightflecks, and their trends correlated with A (Fig. 3I, J). Salt stress increased transient Φ_{PSII} and decreased NPQ largely under lightflecks (Fig. 3I, J).

Photosynthetic oscillation in response to different shadefleck durations and CO_2 partial pressures

After high light (1000 μmol m^{-2} s^{-1})-adapted leaves were exposed to shade (50 μmol m^{-2} s^{-1}) for short durations (1–10 min) and then re-illuminated, A showed strong oscillations in both non-stressed and salt-stressed leaves (Fig. 4). Peak amplitudes compared with the steady state were higher under shorter shadeflecks, and were larger under salt stress compared with control leaves (Figs 4A–D, 5A–C). The time required to achieve steady-state A (settling time) was 4–6 min in control, and consistently reduced by ~2 min in salt-stressed leaves (Fig. 5B). The longer the shadefleck lasted (1–5 min), the longer the settling time tended to be, but after shadeflecks >5 min, the settling time was less affected by shade duration (Fig. 5B). Oscillation frequency showed a negative relationship with settling time, suggesting that the longer a shadefleck lasted (1–5 min), the lower was the frequency; however, again at shadeflecks >5 min, oscillation frequencies were less strongly affected by shade duration (Fig. 5C). Salt stress also increased the oscillation frequency compared with non-stress conditions (Fig. 5C).

At what [CO_2] value do oscillations in A set in, and is their set-in affected by salt stress? We answered these questions by studying photosynthetic oscillation under different [CO_2] (Figs 4I–L, 6). In non-stressed leaves, oscillations were absent at [CO_2]<1000 μbar, but in salt-stress leaves, they were even absent at [CO_2] of 1200 μbar (Fig. 4I–L). Therefore, salt stress increased the [CO_2] threshold at which oscillations first occurred. Under the same [CO_2], salt stress strongly decreased C_i (Fig. 4E–H, M–P) compared with control leaves. In both treatments, the higher the [CO_2], the higher the peak amplitude A and the longer the settling time of A (Fig. 5D, E). Steady-state A followed the same trend as the A–C_i curve (Fig. 7D). There was no significant difference in peak amplitude of A between treatments, but salt stress reduced settling time and increased steady-state A (Fig. 5D–F).

Steady-state leaf photosynthetic properties, carbohydrate, and sucrose phosphate synthase

Salt stress did not significantly affect the light response curve of A, Φ_{PSII}, and NPQ under ambient [CO_2] (Fig. 7). However, salt stress significantly increased A under higher C_i (>600 μbar) compared with control leaves, concomitant with a tendency of lower NPQ (Fig. 7D, F). Salt-stressed leaves had higher TPU than control leaves, but similar maximum rates of carboxylation and electron transport as well as g_m (Table 1). Salt stress did not significantly affect SLA (Table 1).

Salt stress significantly increased sucrose and fructose, but not glucose and starch contents (Fig. 8A). Salt stress did not affect SPS content expressed on either a leaf area or a total protein basis (Fig. 8B, C) and did not stimulate the phosphorylation signal of SPS (Fig. 8D–H).

Discussion

In tomato leaves undergoing photosynthetic induction at high CO_2 partial pressure, prominent photosynthetic oscillations occurred, with salt-stressed leaves showing a fast adjustment to a steady-state, as well as a higher steady-state A after oscillations (Figs 2–5). Below, we discuss the possible mechanisms by which salt stress mitigated these oscillations, and our perspectives on photosynthetic oscillations.

Decreased internal CO_2 partial pressure under salt stress reduces photosynthetic oscillations

Oscillations in A are commonly seen under high [CO_2] and high light intensity. In this study, we observed that after a step increase in light intensity, A oscillated more strongly as [CO_2]

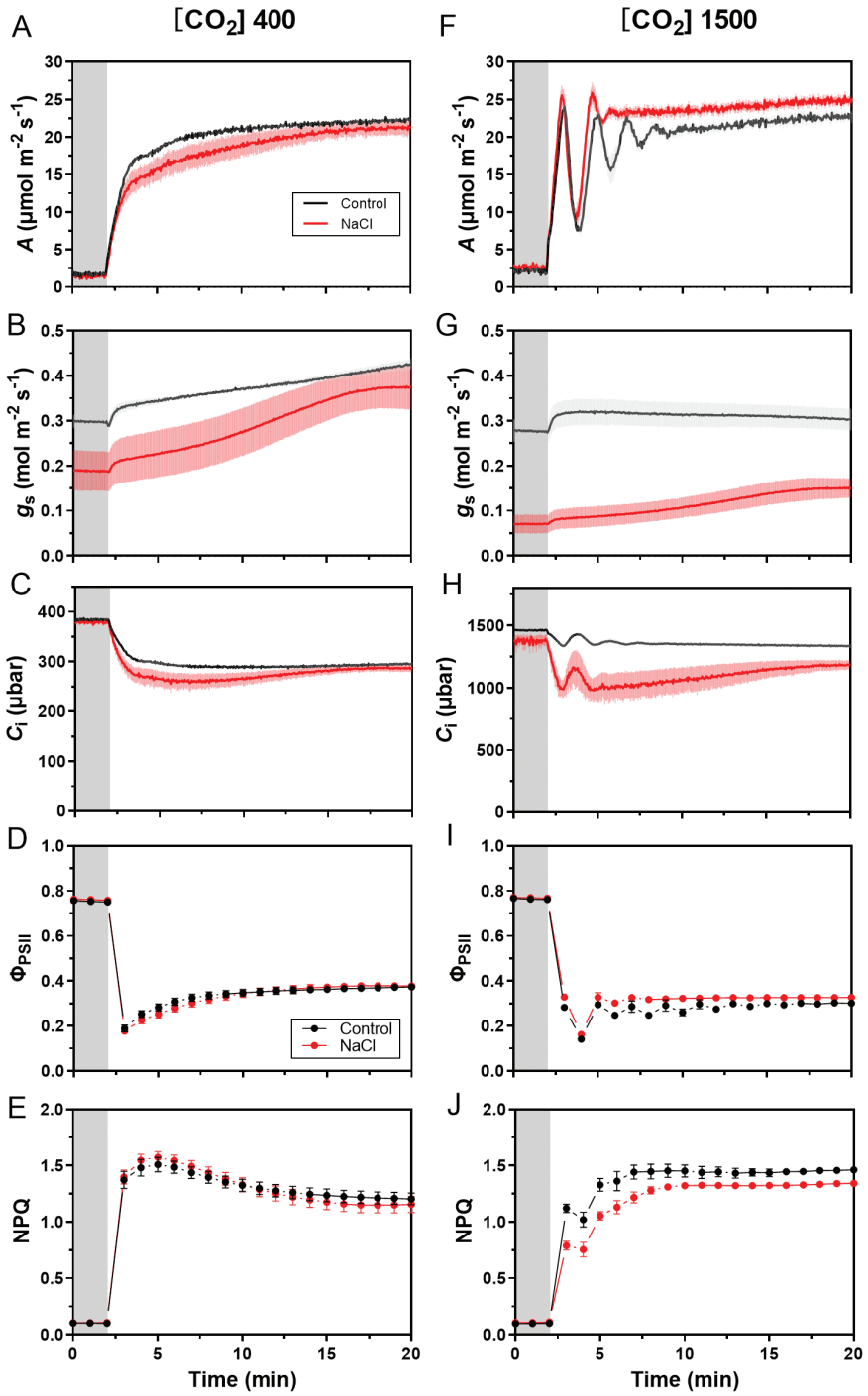

Fig. 2. Time courses of leaf net photosynthetic rate (A; A, F), stomatal conductance (g_s; B, G), leaf internal CO_2 partial pressure (C_i; C, H), photosystem II electron transport efficiency (Φ_{PSII}; D, I), and non-photochemical fluorescence quenching (NPQ; E, J) during photosynthetic induction at air CO_2 partial pressure of 400 and 1500 µbar in tomato leaves. Leaves adapted to low irradiance (50 µmol m^{-2} s^{-1}) were exposed to a step increase in irradiance (1000 µmol m^{-2} s^{-1}). Low and high irradiance are visualized as gray and white backgrounds, respectively. Plants were grown for 10–13 d without NaCl stress (control) or with 100 mM NaCl stress. Data are mean values ±SEM from six plants, grown in two replicate experiments.

increased in the range 800–1500 µbar (Figs 4, 6), in agreement with earlier observations (McVetty and Canvin, 1981; Ogawa, 1982). Two possible reasons could explain why A oscillated more with increased [CO_2]. First, increasing [CO_2] could allow greater CO_2 uptake (Fig. 5D), more readily unbalancing the production and consumption of photosynthetic intermediates (McClain and Sharkey, 2023). Second, increasing [CO_2] decreases the oxygenase activity of Rubisco and subsequent photorespiration (Sharkey,

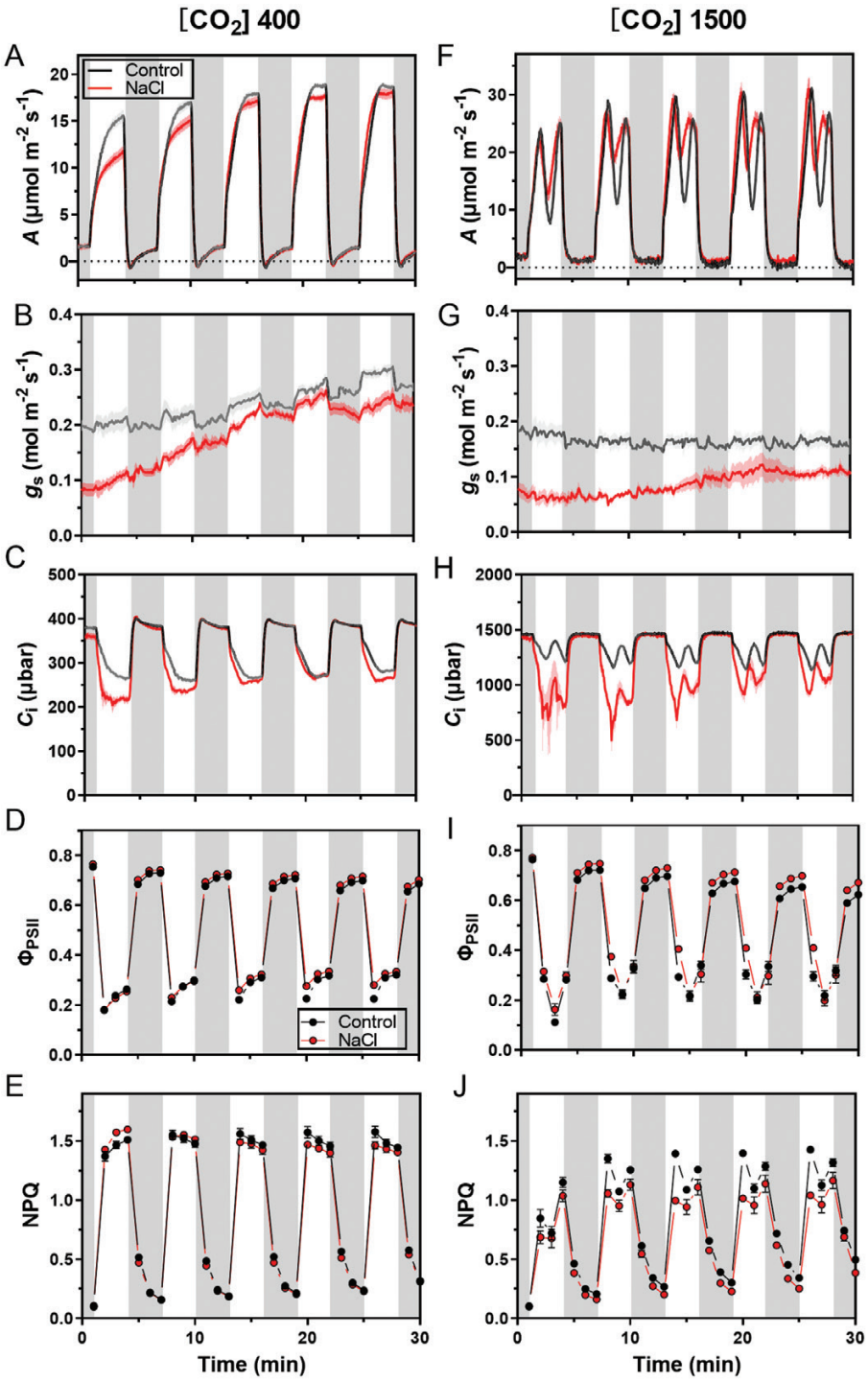

Fig. 3. Time courses of leaf net photosynthetic rate (*A*; A, F), stomatal conductance (g_s; B, G), leaf internal CO_2 partial pressure (C_i; C, H), photosystem II electron transport efficiency (Φ_{PSII}; D, I) and non-photochemical fluorescence quenching (NPQ; E, J) under light fluctuations at air CO_2 partial pressure of 400 and 1500 µbar in tomato leaves. Low irradiance (50 µmol m^{-2} s^{-1})-adapted leaves were exposed to five repeated cycles of 3 min illumination high irradiance (1000 µmol m^{-2} s^{-1}), followed by 3 min of low irradiance (50 µmol m^{-2} s^{-1}). Low and high irradiance are visualized as gray and white backgrounds, respectively. Plants were grown for 10–13 d without NaCl stress (control) or with 100 mM NaCl stress. Data are mean values ±SEM from four to eight plants, grown in two replicate experiments.

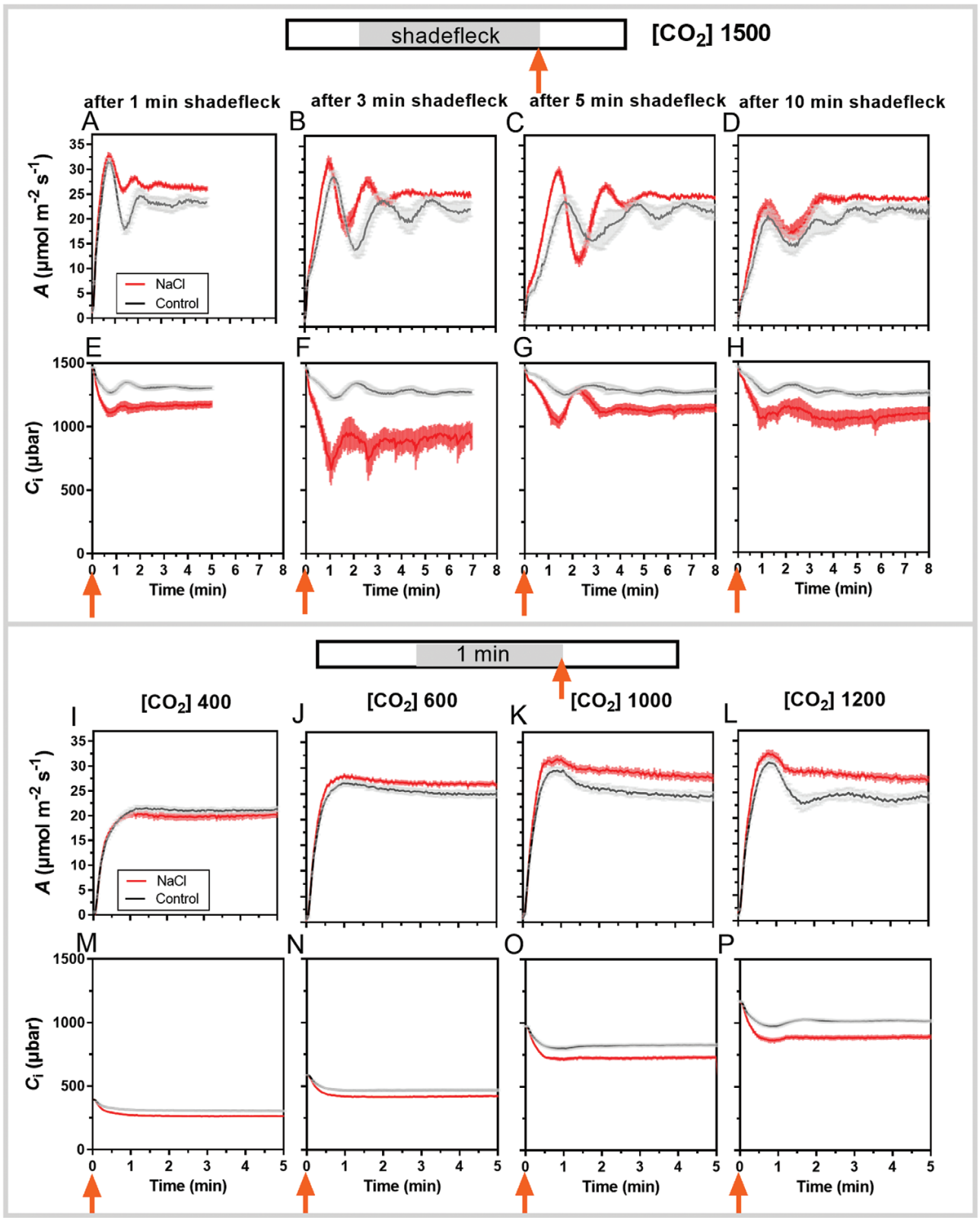

Fig. 4. Time courses of leaf net photosynthetic rate (*A*) and leaf internal CO_2 partial pressure (C_i) after short-term exposure to low irradiance and re-illumination at high irradiance (1000 µmol m^{-2} s^{-1}) in response to different durations of shadefleck (50 µmol m^{-2} s^{-1}, visualized as gray bar above upper panels) at air CO_2 partial pressure of 1500 µbar (A–H) and after re-illumination to high irradiance (1000 µmol m^{-2} s^{-1}) in response to 1 min of shadefleck (50 µmol m^{-2} s^{-1}, visualized as gray bar above lower panels) at different air CO_2 partial pressures ([CO_2] in µbar) (I–P) in tomato leaves. Orange arrows indicate the time when leaves were re-exposed to high irradiance. Plants were grown for 10–13 d without NaCl stress (control) or with 100 mM NaCl stress. Data are mean values ±SEM from 8–11 plants, grown in two replicate experiments.

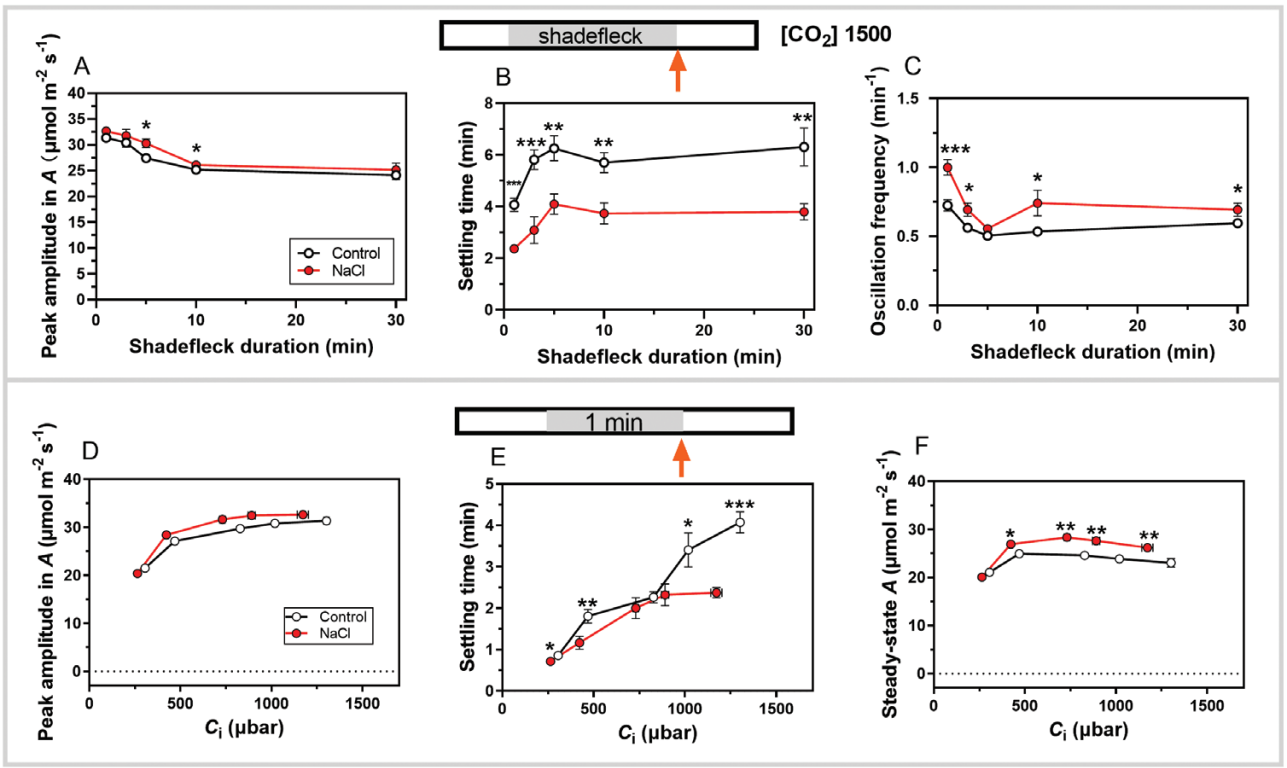

Fig. 5. Key parameters of photosynthetic oscillations after a stepwise increase in irradiance, as affected by shadefleck duration (A–C, shadefleck is visualized as gray bar) and internal CO_2 partial pressure (D–F, shadefleck is visualized as gray bar). *A*, leaf net photosynthetic rate; C_i, leaf internal CO_2 partial pressure. Orange arrows indicate the time when leaves were re-exposed to high irradiance. Plants were grown for 10–13 d without NaCl stress (control) or with 100 mM NaCl stress. Data are mean values ±SEM from 7–11 plants, grown in two replicate experiments. Significance was assessed with Student's *t*-test: **P*<0.05, ***P*<0.01, ****P*<0.001.

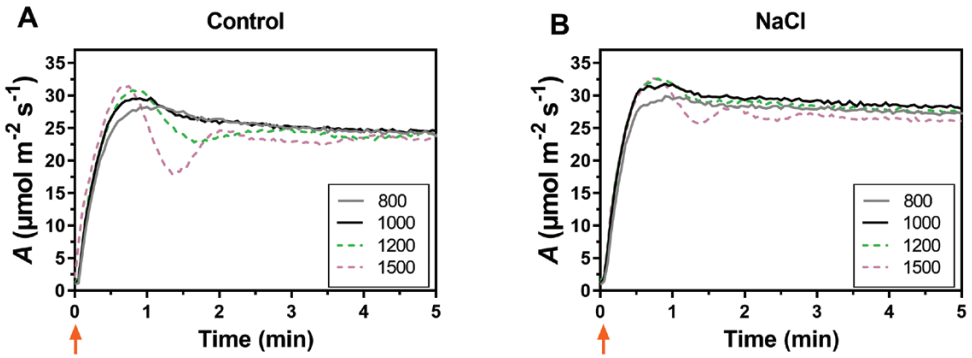

Fig. 6. Time courses of leaf net photosynthetic rate (*A*) after re-illumination to high irradiance (1000 μmol m^{-2} s^{-1}) in response to 1 min of shadefleck (50 μmol m^{-2} s^{-1}) at different air CO_2 partial pressures (in μbar) in tomato leaves. Orange arrows indicate the time when leaves were re-exposed to high irradiance. Data were extracted from Fig. 4A, E–H. Plants were grown for 10–13 d without NaCl stress (control) or with 100 mM NaCl stress. Data are mean values ±SEM from 8–11 plants, grown in two replicate experiments.

1985), leading to more oscillations in *A*. Transferring plants from 20% O_2 to 2% O_2 confirmed the role of photorespiration in inducing oscillations in *A* (Walker *et al.*, 1983; Sharkey *et al.*, 1986). Several hypotheses were proposed: (i) the lack of photorespiration under 2% O_2 could convert pools of photorespiratory intermediates such as glycine and serine to glycerate and then to glycerate-3-phosphate, imposing an additional burden on ATP-generating reactions causing a transient shortage of ATP (Leegood and Furbank, 1986); and (ii) by regulating the redox state of the electron transport chain, photorespiration could promote ATP production, with the lack of photorespiration hampering the regulation of linear and cyclic electron transport, affecting ATP production (McVetty and Canvin, 1981).

Although both salt-stressed and control plants were compared at the same air $[CO_2]$ (C_a), the decrease in g_s under salt stress greatly decreased C_i (Figs 2G, H, 3G, H, 4E–H, M–P). As

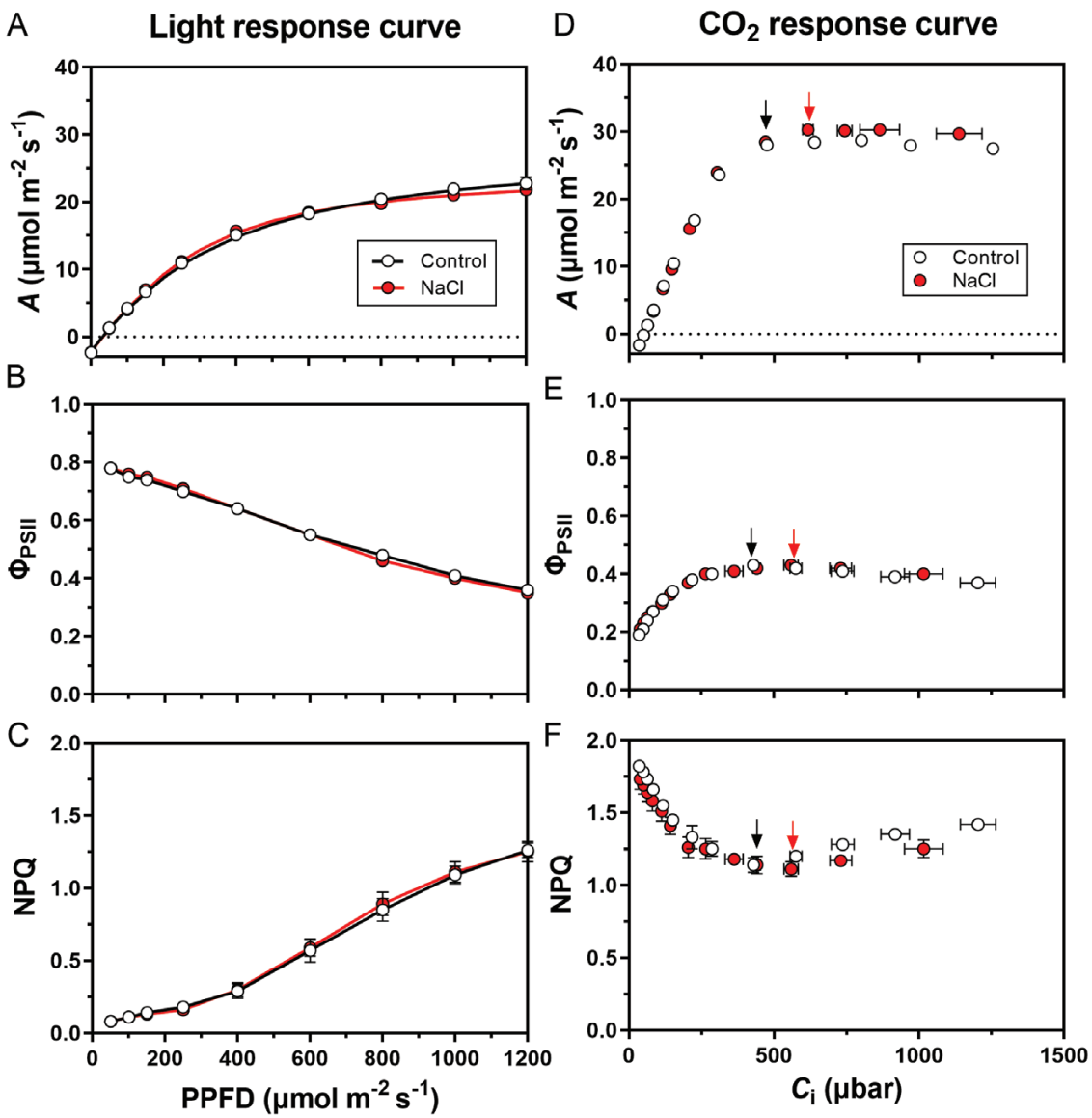

Fig. 7. Steady-state light and CO_2 response curves of leaf photosynthesis in tomato. Responses of leaf net photosynthetic rate (*A*; A, D), photosystem II electron transport efficiency (Φ_{PSII}; B, E) and non-photochemical fluorescence quenching (NPQ; C, F) to incident PPFD and leaf internal CO_2 partial pressure (C_i). Black and red arrows indicated that photosynthesis started to enter TPU limitation at air CO_2 partial pressure of 600 μbar in control leaves and 1000 μbar in NaCl-stressed leaves. Plants were grown for 10–13 d without NaCl stress (control) or with 100 mM NaCl stress. Data are mean values ±SEM from four plants, grown in two replicate experiments.

Table 1. Parameters characterizing steady-state photosynthesis and leaf thickness

Treatment	R_d (μmol m^{-2} s^{-1})	α (μmol μmol $^{-1}$)	A_{max} (μmol m^{-2} s^{-1})	V_{cmax} (μmol m^{-2} s^{-1})	J_{1000} (μmol m^{-2} s^{-1})	TPU (μmol m^{-2} s^{-1})	g_m (mol m^{-2} s^{-1})	SLA (cm^2 g^{-1})
Control	2.2	0.071	30.5	122	168	**8.6**	0.16	314.6
NaCl	2.3	0.071	26.9	115	166	**9.4**	0.15	305.5
P	0.62	0.98	0.23	0.28	0.67	**0.003**	0.43	0.73

Plants were grown for 10–13 d without NaCl stress (control) or with 100 mM NaCl stress. Mean values from 4~6 plants, grown in two separate experiments, are shown. *P*-values for the NaCl stress effect are shown (Student's *t*-test). Values shown in bold indicate significant difference. α, quantum yield; A_{max}, light-saturated net photosynthesis rate; g_m, mesophyll conductance; J_{1000}, electron transport rate at light intensity of 1000 μmol m^{-2} s^{-1}; R_d, dark respiration; SLA, specific leaf area; TPU, triose phosphate use rate; V_{cmax}, maximum carboxylation rate.

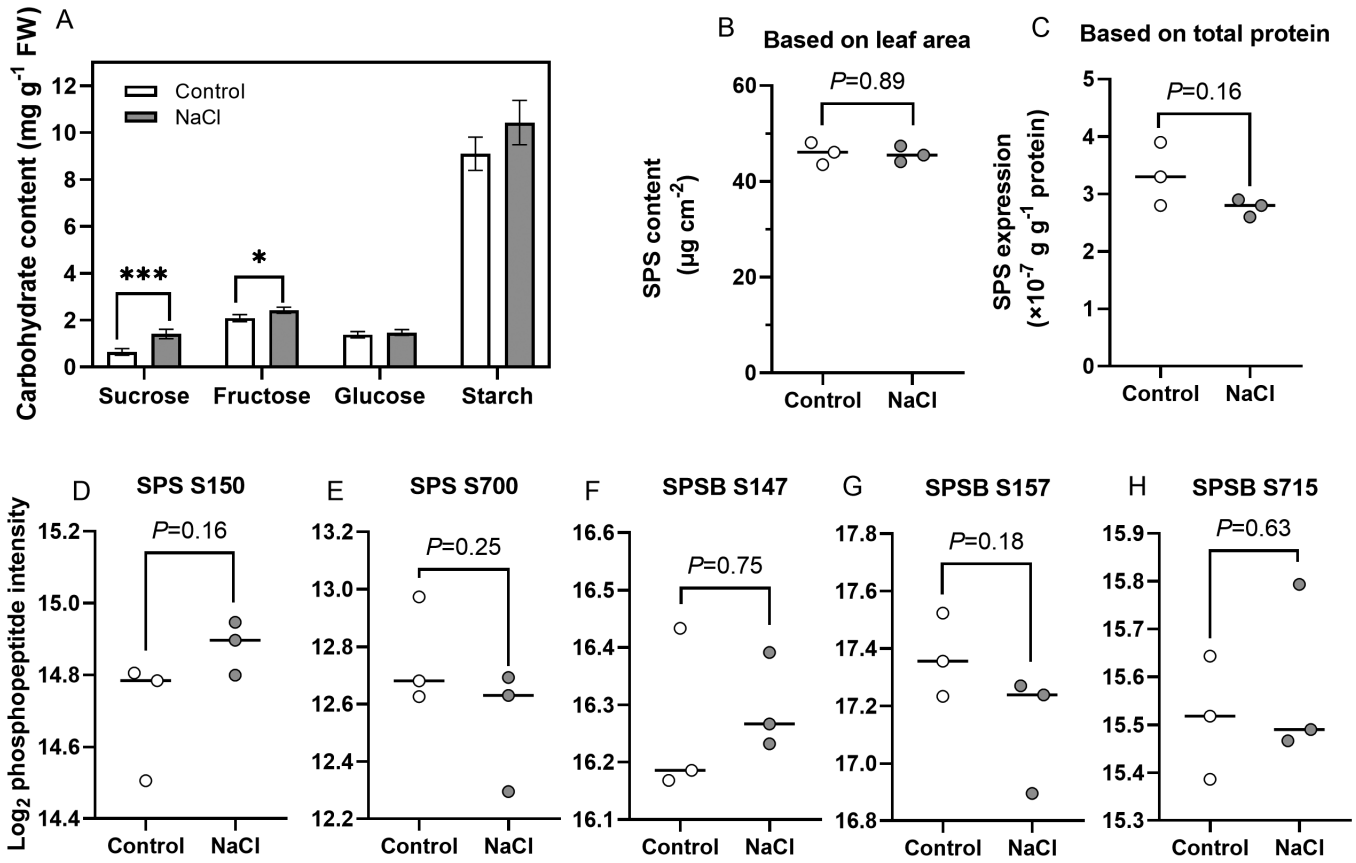

Fig. 8. Effects of NaCl stress on carbohydrate content (A), sucrose phosphate synthase (SPS) content (B, C), and phosphorylated SPS signals (five phosphorylates sites in SPS, D–H) in tomato leaves. Plants were grown for 10–13 d without NaCl stress (control) or with 100 mM NaCl stress. Data in (A) are mean values ±SEM from 10 plants, grown in two replicate experiments. Significance was assessed with Student's *t*-test: **P*<0.05, ****P*<0.001. Bar diagrams (B–H) with individual values show the mean from three biological replicates in each treatment.

the mesophyll conductance (g_m) was similar between treatments (Table 1), [CO_2] at the carboxylation site (C_c) was likely lower in salt-stressed plants than non-stressed plants. As discussed above, increasing [CO_2] caused greater oscillations in A, while at the same C_a, decreases in C_i or C_c under salt stress attenuated oscillations in A. Indeed, when control and salt-stressed leaves had similar C_i (e.g. at a C_a of 1000 µbar in control (Fig. 4O) but a C_a of 1200 µbar in salt stressed leaves (Fig. 4P)), the time course of A was very similar (control in Fig. 4K and salt stress in Fig. 4L). Therefore, the decrease in C_i may play a key role in reducing A oscillations under salt stress. However, the settling time of oscillations was reduced by ~2 min across all shadefleck durations in salt-stressed leaves, even at a C_i that was much higher than in control leaves (Fig. 5B). This suggests other reasons could attenuate photosynthetic oscillations under salt stress.

High triose-phosphate utilization capacity may reduce photosynthetic oscillations under salt stress

TPU limitation reflects a condition in which A is limited by the ability to regenerate P_i, by producing end products of photosynthesis (McClain and Sharkey, 2019). In other words, TPU can be used to estimate the maximum rate of end-product synthesis within a leaf. A short-term (10–13 d) salt stress increased steady-state TPU capacity in tomato leaves (Fig. 7D; Table 1) as observed previously (Zhang *et al.*, 2018; Y. Zhang *et al.*, 2022). This increased the rate of P_i-cycling from the cytosol to the chloroplast, thereby maintaining a high A. Feeding cytosolic P_i through the transpiration stream decreased these oscillations and increased the threshold for light intensity and [CO_2] at which photosynthetic oscillations occurred (Laisk and Walker, 1986; Stitt and Schreiber, 1988). As the short-term salt stress increased TPU capacity without affecting maximum Rubisco carboxylation and electron transport rates, we assume it could also increase the rate of P_i-cycling from the cytosol to the chloroplast, thereby attenuating photosynthetic oscillations (Figs 4, 5).

Sucrose synthesis capacity is a key regulator of TPU (Yang *et al.*, 2016; McClain and Sharkey, 2019). Inhibiting sucrose synthesis may limit export of TP from the chloroplast, decreasing cytosolic P_i and TPU (Paul and Pellny, 2003). SPS, which catalyses the last step of cytoplasmic sucrose synthesis, is a key

regulatory enzyme in sucrose synthesis (Cheikh *et al.*, 1992; Huber and Huber, 1992). However, the increase in TPU capacity was not linked to an increased SPS activity in this study (Fig. 8B–H). Acclimation to salt stress did not affect how quickly sucrose synthesis deactivated in shade or activated during subsequent high light exposure, as salt stress did not affect the relationship between settling time versus shadefleck duration (Fig. 5B). Thus, acclimation to salt stress does not seem to affect light-activation or shade-deactivation rates nor the steady-state activity of SPS. Other possibilities for increased TPU are a higher activity or concentration of chloroplast fructose-2,6-bisphosphate (Stitt *et al.*, 1984), as well as an increase in P_i transporters (thylakoid membrane localized PHT4;1 and inner envelope localized PHT4;4 and PHT4;5; see Finazzi *et al.*, 2015; Karlsson *et al.*, 2015). These P_i transporters use Na^+ as the co-transporting ion to regulate Na^+ and P_i concentrations inside the chloroplast under salt stress (Bose *et al.*, 2017). If P_i transporters were up-regulated, they may increase chloroplast P_i concentrations, which can facilitate ATP synthase to produce ATP and mitigate photosynthetic oscillations. How these P_i transporters are regulated during salt stress is unknown.

As the duration of salt stress lasted 13 d, carbon partitioning and sugar metabolism were likely stable, with increased leaf sucrose content helping to maintain osmotic balance both inside and outside the cell. Sucrose accumulation can lead to a feedback inhibition of photosynthesis, through signaling by trehalose-6-phosphate (Chang *et al.*, 2017; Paul *et al.*, 2020). However, in this study, a large increase in sucrose content under salt stress (Fig. 8A) did not measurably decrease A (Fig. 7) but instead occurred concomitantly with an increased TPU capacity (Table 1). This phenomenon may be explained by high cytoplasmic sucrose concentrations, which are thought to be relatively constant throughout the photoperiod, with net accumulation restricted to the vacuole (Weiner *et al.*, 1992; Winter and Huber, 2000). In other words, the large amounts of sucrose in salt stressed leaves may be localized to the vacuole, meaning they would not directly inhibit A in the cytoplasm. Tomato's tolerance of end-product inhibition (Chang *et al.*, 2017) could be due to its large sink growth potential and low sensitivity of its SPS to carbohydrate accumulation (Huber and Huber, 1996).

Non-steady state measurements allow insights into the regulation of photosynthesis under salt stress

Several enzymes in end-product synthesis deactivate in the shade and activate under high light intensities (Stitt and Grosse, 1988; Huber and Huber, 1992), similar to several enzymes in the CBB cycle (e.g. fructose-1,6-bisphosphatase, sedohepturose-1,7-bisphosphatase, pyruvate phosphate dikinase, Rubisco). The activation state of SPS depends on the kinetics of protein dephosphorylation and phosphorylation (Huber and Huber, 1992; Jones *et al.*, 1998), which is relevant during photosynthetic oscillations (Laisk and Walker, 1986). Mathematical models indicated that the modulation of sucrose synthesis proceeded with a time lag of about 15–20 s, thereby causing damped oscillations in A (Laisk and Walker, 1986). When exposure to low light increased from 1 min to 5 min, tomato leaves required more time until photosynthetic oscillations had settled, but this duration did not change with longer shade exposure (Fig. 5B). These results suggest that although sucrose and/or starch synthesis had reached a less activated state under low light of >5 min, rates of synthesis could become fully operational within 6 min of high light (settling time in control was ~6 min after 5–30 min of shadefleck; Fig. 8B). Activation rates of sucrose synthesis from low light intensity are thus in the same range as those of Rubisco, which has time constants of 3–7 min during photosynthetic induction (Kaiser *et al.*, 2018). Previous *in vivo* studies on spinach and barley showed that after a dark-to-light transition, SPS is usually fully activated in 5–15 min, and dark-inactivated within 20–30 min (Huber *et al.*, 1989; Weiner *et al.*, 1992). Because photosynthesis still proceeds under low light intensity, full activation of SPS from the shade may take much less time than from darkness. However, light modulation of SPS is not conserved among species: some species exhibit a marked light activation and dark (or shade) deactivation of SPS (e.g. maize, barley, spinach, sugar beet, tomato), whereas others show little light/dark modulation of SPS activity (e.g. soybean, pea, tobacco, Arabidopsis, cucumber) (Huber *et al.*, 1989; Huber and Huber, 1996; Jones and Ort, 1997). For the latter species, SPS probably remains active under low light, and might have reduced effects on photosynthesis after a longer shade period (e.g. >5 min). To generalize the role of light modulation of SPS on dynamic photosynthesis, more species should be surveyed. Moreover, clarifying the basis for the lack of light activation of SPS in some species, which is still unresolved, is important.

Despite the sudden drop of A, shadeflecks can still cause P_i release due to ongoing sugar and starch synthesis, as well as other minor metabolic processes such as amino acid and isoprenoid synthesis (McClain and Sharkey, 2019). High light intensity illumination causes A to transiently peak during oscillations, representing the maximum attainable RuBP regeneration rate and a transient maximum pool size of metabolites in the CBB cycle. Normally, the rate of RuBP regeneration increases with a rise in $[CO_2]$, as illustrated by the Farquhar–von Caemmerer–Berry model (Farquhar *et al.*, 1980), and the peak value of A during oscillations also followed the same trend when plotted against C_i (Fig. 5D). Photosynthesis should be able to transiently exceed the RuBP regeneration-limited portion of the A–C_i curve, if RuBP is initially in excess, and peak height would then be related to the size of the available metabolite pool (McClain and Sharkey, 2023). Peak values of A were ~32 μmol m^{-2} s^{-1} in both control and salt-stressed leaves (Fig. 5D), suggesting that salt stress did not negatively affect the pool size of available carbon metabolites.

Studying photosynthesis under triose phosphate utilization limitation combined with salt stress is relevant to understanding

environmental regulation of photosynthesis in coastal ecosystems and some irrigated areas where plants experience substantial salt stress. However, we only studied TPU limitation by supplying transient increases (<1 h) in both light intensity and [CO_2] in plants grown under current air [CO_2] and constant low light intensity (200 μmol m^{-2} s^{-1}). Based on a recent study, we could speculate that after some period of high [CO_2] acclimation (>1 d), both salt-stressed and non-stressed plants that were initially TPU-limited will eventually not be TPU-limited, with decreasing maximum rates of carboxylation and electron transport regulating *A* (McClain *et al.*, 2023). In plants acclimated to different [CO_2] and light intensities, we speculate that a new balance of photosynthetic control will establish, which may differ between salt-stressed and non-stressed plants. Future studies should examine the combination of [CO_2] and salt stress on TPU regulation, which will be relevant for future climate scenarios.

Conclusions

During photosynthetic induction under high CO_2 partial pressure, salt stress strongly reduced photosynthetic oscillations of tomato leaves. This reduction was most likely due to stomatal closure decreasing internal CO_2 partial pressure and an increased TPU capacity, facilitating phosphate-cycling from the cytosol to the chloroplast. Our results provide new insights into how CO_2 availability and end-product synthesis modulate photosynthesis of salt-stressed plants.

Acknowledgements

We thank Dr Jie Zou for help with sugar content measurements and Bo Zhou for guidance on data analysis.

Author contributions

YZ, EK, and TL conceived and designed the research; YZ performed the experiments; YZ and SD analysed the data with suggestions from all other authors; YZ wrote the manuscript; all authors reviewed and edited the article, and endorsed its final version.

Conflict of interest

The authors declare they have no conflict of interest.

Funding

This work was supported by the National Natural Science Foundation of China (no. 32102465; no. 32172654), the Young Elite Scientists Sponsorship Program by CAST (2022QNRC001), and the Central Public-interest Scientific Institution Basal Research Fund (no. BSRF202201 no. BSRF202310).

Data availability

All data supporting the findings of this study are available within the paper.

References

Bose J, Munns R, Shabala S, Gilliham M, Pogson B, Tyerman SD. 2017. Chloroplast function and ion regulation in plants growing on saline soils: lessons from halophytes. Journal of Experimental Botany **68**, 3129–3143.

Cannell MGR, Thornley JGM. 1998. Temperature and CO_2 responses of leaf and canopy photosynthesis: A clarification using the non-rectangular hyperbola model of photosynthesis. Annals of Botany **82**, 883–892.

Chang TG, Zhu XG, Raines C. 2017. Source–sink interaction: a century old concept under the light of modern molecular systems biology. Journal of Experimental Botany **68**, 4417–4431.

Chaves MM, Costa JM, Saibo NJ. 2011. Recent advances in photosynthesis under drought and salinity. Advances in Botanical Research **57**, 49–104.

Cheikh N, Brenner ML, Huber JL, Huber SC. 1992. Regulation of sucrose phosphate synthase by gibberellins in soybean and spinach plants. Plant Physiology **100**, 1238–1242.

Dartora N, de Souza LM, Santana-Filho AP, Iacomini M, Valduga AT, Gorin PAJ, Sassaki GL. 2011. UPLC-PDA–MS evaluation of bioactive compounds from leaves of *Ilex paraguariensis* with different growth conditions, treatments and ageing. Food Chemistry **129**, 1453–1461.

Dietz KJ, Hell R. 2015. Thiol switches in redox regulation of chloroplasts: balancing redox state, metabolism and oxidative stress. Biological Chemistry **396**, 483–494.

Farquhar GD, von Caemmerer S, Berry J. 1980. A biochemical model of photosynthetic CO_2 assimilation in leaves of C_3 species. Planta **149**, 78–90.

Finazzi G, Petroutsos D, Tomizioli M, Flori S, Sautron E, Villanova V, Rolland N, Seigneurin-Berny D. 2015. Ions channels/transporters and chloroplast regulation. Cell Calcium **58**, 86–97.

Fridlyand L. 1998. Independent changes of ATP/ADP or ΔpH could cause oscillations in photosynthesis. Journal of Theoretical Biology **193**, 739–741.

Furbank RT, Walker DA. 1985. Photosynthetic induction in C_4 leaves an investigation using infra-red gas analysis and chlorophyll a fluorescence. Planta **163**, 75–83.

Giersch C. 1986. Oscillatory response of photosynthesis in leaves to environmental perturbations: a mathematical model. Archives of Biochemistry and Biophysics **245**, 263–270.

Harley PC, Loreto F, di Marco G, Sharkey TD. 1992. Theoretical considerations when estimating the mesophyll conductance to CO_2 flux by analysis of the response of photosynthesis to CO_2. Plant Physiology **98**, 1429–1436.

Huber SC, Huber JL. 1992. Role of sucrose-phosphate synthase in sucrose metabolism in leaves. Plant Physiology **99**, 1275–1278.

Huber SC, Huber JL. 1996. Role and regulation of sucrose-phosphate synthase in higher plants. Annual Review of Plant Physiology and Plant Molecular Biology **47**, 431–444.

Huber SC, Nielsen TH, Huber JL, Pharr DM. 1989. Variation among species in light activation of sucrose-phosphate synthase. Plant & Cell Physiology **30**, 277–285.

Jones TL, Ort DR. 1997. Circadian regulation of sucrose phosphate synthase activity in tomato by protein phosphatase activity. Plant Physiology **113**, 1167–1175.

Jones TL, Tucker DE, Ort DR. 1998. Chilling delays circadian pattern of sucrose phosphate synthase and nitrate reductase activity in tomato. Plant Physiology **118**, 149–158.

Kaiser E, Kromdijk J, Harbinson J, Heuvelink E, Marcelis LF. 2017a. Photosynthetic induction and its diffusional, carboxylation and electron

transport processes as affected by CO_2 partial pressure, temperature, air humidity and blue irradiance. Annals of Botany **119**, 191–205.

Kaiser E, Morales A, Harbinson J. 2018. Fluctuating light takes crop photosynthesis on a rollercoaster ride. Plant Physiology **176**, 977–989.

Kaiser E, Morales A, Harbinson J, Kromdijk J, Heuvelink E, Marcelis LF. 2015. Dynamic photosynthesis in different environmental conditions. Journal of Experimental Botany **66**, 2415–2426.

Kaiser E, Zhou D, Heuvelink E, Harbinson J, Morales A, Marcelis LFM, Sharwood R. 2017b. Elevated CO_2 increases photosynthesis in fluctuating irradiance regardless of photosynthetic induction state. Journal of Experimental Botany **68**, 5629–5640.

Karlsson PM, Herdean A, Adolfsson L, *et al*. 2015. The *Arabidopsis* thylakoid transporter PHT4;1 influences phosphate availability for ATP synthesis and plant growth. The Plant Journal **84**, 99–110.

Laisk A, Eichelmann H. 1989. Towards understanding oscillations: a mathematical model of the biochemistry of photosynthesis. Philosophical Transactions of the Royal Society of London. B, Biological Sciences **323**, 369–384.

Laisk A, Eichelmann H, Oja V, Eatherall A, Walker DA. 1989. A mathematical model of the carbon metabolism in photosynthesis. Difficulties in explaining oscillations by fructose 2,6-bisphosphate regulation. Proceedings of the Royal Society B **237**, 389–415.

Laisk A, Siebke K, Gerst U, Eichelmann H, Oja V, Heber U. 1991. Oscillations in photosynthesis are initiated and supported by imbalances in the supply of ATP and NADPH to the Calvin cycle. Planta **185**, 554–562.

Laisk A, Walker DA. 1986. Control of phosphate turnover as a rate-limiting factor and possible cause of oscillations in photosynthesis: a mathematical model. Proceedings of the Royal Society B **227**, 281–302.

Leegood RC, Furbank R. 1986. Stimulation of photosynthesis by 2% oxygen at low temperatures is restored by phosphate. Planta **168**, 84–93.

Liu T, Barbour MM, Yu D, Rao S, Song X. 2022. Mesophyll conductance exerts a significant limitation on photosynthesis during light induction. New Phytologist **233**, 360–372.

Loriaux SD, Avenson TJ, Welles JM, McDermitt DK, Eckles RD, Riensche B, Genty B. 2013. Closing in on maximum yield of chlorophyll fluorescence using a single multiphase flash of sub-saturating intensity. Plant, Cell & Environment **36**, 1755–1770.

McClain AM, Cruz JA, Kramer DM, Sharkey TD. 2023. The time course of acclimation to the stress of triose phosphate use limitation. Plant, Cell & Environment **46**, 64–75.

McClain AM, Sharkey TD. 2019. Triose phosphate utilization and beyond: from photosynthesis to end product synthesis. Journal of Experimental Botany **70**, 1755–1766.

McClain AM, Sharkey TD. 2023. Rapid CO_2 changes cause oscillations in photosynthesis that implicate PSI acceptor-side limitations. Journal of Experimental Botany **74**, 3163–3173.

McVetty PBE, Canvin DT. 1981. Inhibition of photosynthesis by low oxygen concentrations. Canadian Journal of Botany **59**, 721–725.

Ogawa T. 1982. Simple oscillations in photosynthesis of higher plants. Biochimica et Biophysica Acta **681**, 103–109.

Paul MJ, Pellny TK. 2003. Carbon metabolite feedback regulation of leaf photosynthesis and development. Journal of Experimental Botany **54**, 539–547.

Paul MJ, Watson A, Griffiths CA. 2020. Trehalose 6-phosphate signalling and impact on crop yield. Biochemical Society Transactions **48**, 2127–2137.

Rasulov B, Talts E, Niinemets U. 2016. Spectacular oscillations in plant isoprene emission under transient conditions explain the enigmatic CO_2 response. Plant Physiology **172**, 2275–2285.

Rogers A, Kumarathunge DP, Lombardozzi D, Medlyn BE, Serbin SP, Walker AP. 2021. Triose phosphate utilization limitation: an unnecessary complexity in terrestrial biosphere model representation of photosynthesis. New Phytologist **230**, 17–22.

Sage R, Sharkey TD, Seemann JR. 1988. The in-vivo response of the ribulose-1,5-bisphosphate carboxylase activation state and the pool sizes of photosynthetic metabolites to elevated CO_2 in *Phaseolus vulgaris* L. Planta **174**, 407–416.

Salter WT, Merchant AM, Richards RA, Trethowan R, Buckley TN. 2019. Rate of photosynthetic induction in fluctuating light varies widely among genotypes of wheat. Journal of Experimental Botany **70**, 2787–2796.

Schurr U, Walter A, Rascher U. 2006. Functional dynamics of plant growth and photosynthesis – from steady-state to dynamics – from homogeneity to heterogeneity. Plant, Cell and Environment **29**, 340–352.

Sharkey TD. 1985. O_2-insensitive photosynthesis in C_3 plants: its occurrence and a possible explanation. Plant Physiology **78**, 71–75.

Sharkey TD. 2016. What gas exchange data can tell us about photosynthesis. Plant, Cell & Environment **39**, 1161–1163.

Sharkey TD, Bernacchi CJ, Farquhar GD, Singsaas EL. 2007. Fitting photosynthetic carbon dioxide response curves for C_3 leaves. Plant, Cell & Environment **30**, 1035–1040.

Sharkey TD, Stitt M, Heineke D, Gerhardt R, Raschke K, Heldt HW. 1986. Limitation of photosynthesis by carbon metabolism: II. O_2-insensitive CO_2 uptake results from limitation of triose phosphate utilization. Plant Physiology **81**, 1123–1129.

Siebke K, Weis E. 1995. Imaging of chlorophyll-*a*-fluorescence in leaves: Topography of photosynthetic oscillations in leaves of *Glechoma hederacea*. Photosynthesis Research **45**, 225–237.

Sivak MN, Dietz KJ, Heber U, Walker D. 1985. The relationship between light scattering and chlorophyll *a* fluorescence during oscillations in photosynthetic carbon assimilation. Archives of Biochemistry and Biophysics **237**, 513–519.

Stirbet A, Riznichenko GY, Rubin AB, Govindjee. 2014. Modeling chlorophyll a fluorescence transient: relation to photosynthesis. Biochemistry **79**, 291–323.

Stitt M, Grosse H. 1988. Interactions between sucrose synthesis and CO_2 fixation I. secondary kinetics during photosynthetic induction are related to a delayed activation of sucrose synthesis. Journal of Plant Physiology **133**, 129–137.

Stitt M, Kurzel B, Heldt HW. 1984. Control of photosynthetic sucrose synthesis by fructose 2,6-bisphosphate: II. Partitioning between sucrose and starch. Plant Physiology **75**, 554–560.

Stitt M, Schreiber U. 1988. Interaction between sucrose synthesis and CO_2 fixation III. Response of biphasic induction kinetics and oscillations to manipulation of the relation between electron transport, Calvin cycle, and sucrose synthesis. Journal of Plant Physiology **133**, 263–271.

Szecowka M, Heise R, Tohge T, *et al*. 2013. Metabolic fluxes in an illuminated *Arabidopsis* rosette. The Plant Cell **25**, 694–714.

Van der Veen R. 1949. Induction phenomena in photosynthesis. I. Physiologia Plantarum **2**, 217–234.

Walker DA. 1992. Concerning oscillations. Photosynthesis Research **34**, 387–395.

Walker DA, Sivak MN, Prinsley RT, Cheesbrough JK. 1983. Simultaneous measurement of oscillations in oxygen evolution and chlorophyll *a* fluorescence in leaf pieces. Plant Physiology **73**, 542–549.

Weiner H, McMichael RW, Huber SC. 1992. Identification of factors regulating the phosphorylation status of sucrose-phosphate synthase *in vivo*. Plant Physiology **99**, 1435–1442.

Winter H, Huber SC. 2000. Regulation of sucrose metabolism in higher plants: localization and regulation of activity of key enzymes. Critical Reviews in Biochemistry and Molecular Biology **35**, 253–289.

Wungrampha S, Joshi R, Singla-Pareek S, Pareek A. 2018. Photosynthesis and salinity: are these mutually exclusive? Photosynthetica **56**, 366–381.

Yang JT, Preiser AL, Li Z, Weise SE, Sharkey TD. 2016. Triose phosphate use limitation of photosynthesis: short-term and long-term effects. Planta **243**, 687–698.

Yue J, Shi D, Zhang L, Zhang Z, Fu Z, Ren Q, Zhang J. 2020. The photo-inhibition of camphor leaves (*Cinnamomum camphora* L.) by NaCl

stress based on physiological, chloroplast structure and comparative proteomic analysis. PeerJ **8**, e9443.

Zhang N, Berman S, Joubert D, Vialet-Chabrand S, Marcelis LFM, Kaiser E. 2022. Variation of photosynthetic induction in major horticultural crops is mostly driven by differences in stomatal traits. Frontiers in Plant Science **13**, 860229.

Zhang Y, Kaiser E, Li T, Marcelis LFM. 2022. NaCl affects photosynthetic and stomatal dynamics by osmotic effects and reduces photosynthetic capacity by ionic effects in tomato. Journal of Experimental Botany **73**, 3637–3650.

Zhang Y, Kaiser E, Zhang Y, Yang Q, Li T. 2018. Short-term salt stress strongly affects dynamic photosynthesis, but not steady-state photosynthesis, in tomato (*Solanum lycopersicum*). Environmental and Experimental Botany **149**, 109–119.

Zorb C, Geilfus CM, Dietz KJ. 2019. Salinity and crop yield. Plant Biology **21**, 31–38.